Quantum-enhanced accelerometry with a nonlinear electromechanical circuit

Kurt Jacobs,[1,2,3] Radhakrishnan Balu,[1,4] and John D. Teufel[5]

[1]*U.S. Army Research Laboratory, Computational and Information Sciences Directorate, Adelphi, Maryland 20783, USA*
[2]*Department of Physics, University of Massachusetts at Boston, Boston, Massachusetts 02125, USA*
[3]*Hearne Institute for Theoretical Physics, Louisiana State University, Baton Rouge, Louisiana 70803, USA*
[4]*Computer Science and Electrical Engineering, 1000 Hilltop Circle, Baltimore, Maryland 21250, USA*
[5]*National Institute of Standards and Technology, Boulder, Colorado 80305, USA*

It is known that placing a mechanical oscillator in a superposition of coherent states allows, in theory, a measurement of a linear force whose sensitivity increases with the amplitude of the mechanical oscillations, a uniquely quantum effect. Further, entangled versions of these states across a network of n mechanical oscillators enable a measurement whose sensitivity increases linearly with n, thus improving the classical scaling by $\sqrt{n}$. One of the key challenges in exploiting this effect is processing the signal so that it can be readily measured; linear processing is insufficient. Here we show that a Kerr oscillator will not only create the necessary states, but also perform the required processing, transforming the quantum phase imprinted by the force signal into a shift in amplitude measurable with homodyne detection. This allows us to design a relatively simple quantum electromechanical circuit that can demonstrate the core quantum effect at the heart of this scheme, namely amplitude-dependent force sensitivity. We derive analytic expressions for the performance of the circuit, including thermal mechanical noise and photon loss. We discuss the experimental challenges in implementing the scheme with near-term technology.

I. INTRODUCTION

The uniquely quantum-mechanical properties of mesoscopic systems have the potential to improve sensors far beyond what is possible with classical devices [1–4]. This potential is one of the driving forces in the development of controllable quantum systems [5–25]. Here we present a relatively simple superconducting circuit, consisting of two superconducting nonlinear oscillators coupled to a nanomechanical resonator, that can be used to harness the ability of superpositions of coherent states to perform accelerometry in a uniquely quantum-enabled manner. The requirements for implementing this circuit are not far from present technology; the required components have been demonstrated in recent experiments [26–30].

To understand the difference between quantum and classical force detection, the first thing to note is that the accuracy of a classical force measurement is not affected in any way by the energy of the oscillator used to detect the force. The reason for this is that the amount by which an applied force causes the position and momentum of an oscillator to deviate from their free evolution is independent of their initial values. Consider an oscillator with frequency ω driven by a resonant force $F(t) = F \cos(\omega t)$. Denoting the (dimensionless) position and momentum of the oscillator by x and p, respectively, the free evolution of the (undamped) oscillator in phase space is merely a rotation about the origin. Moving into this rotating frame, and assuming that the damping rate of the oscillator is small compared to ω, the action of the force is merely to shift the momentum of the oscillator by an amount proportional to Ft in which t is time. The signal is the shift in p, and since this transforms back and forth between x and p due to the rotation in phase space, the force is usually measured by measuring the resulting shift in x. The initial energy of the resonator thus has no effect on the sensitivity of the force measurement. Note

that this is very different from the measurement of a phase shift. A phase shift causes a displacement in phase space equal to the phase shift multiplied by the initial amplitude of the resonator, and so the signal is proportional to the square root of the oscillator's energy.

It turns out that a remarkable property of quantum mechanics provides a means to measure a force via an oscillator in a way in which the signal induced by the force is proportional to the square root of the energy. As a result, the accuracy of the measurement can be increased by increasing the amplitude of the oscillator's initial state. This effect can be achieved by preparing the oscillator in a superposition of two coherent states. Such states, in which a mechanical oscillator is in "two places at the same time," are often referred to as "cat" states, and they have been generated in electrical oscillators using a Kerr nonlinearity [31,32]. The difference between quantum and classical systems under the influence of a force is that while both undergo a shift in phase space, a quantum system is subject to a second distinct kind of change, being a change to the phase of the state. In particular, the action of a force $F(t) = \cos(\omega t)$ over a time Δt on a coherent state $|\alpha\rangle$ (in the frame rotating with the oscillator) is given by

$$e^{-iFx\,\Delta t/\hbar}|\alpha\rangle = e^{i\,\mathrm{Re}[\alpha]\delta}|\alpha + i\delta\rangle, \qquad (1)$$

where δ is the induced momentum shift in units of the dimensionless momentum, $\tilde{p}$:

$$\delta = \frac{F\Delta t}{\sqrt{2m\omega\hbar}}, \qquad (2)$$

$$\tilde{p} = -i(a - a^{\dagger}). \qquad (3)$$

The shift induced in phase space is the same as that for a classical oscillator and is given by δ, whereas the shift to the global phase of the coherent state is $\delta\,\mathrm{Re}[\alpha]$. Unlike the shift in phase space, this shift is proportional to $\mathrm{Re}[\alpha]$ and thus to

the amplitude of the oscillator. While the global phase of a quantum state has no physical meaning in itself, the induced phase shift becomes observable when the state of the oscillator is a superposition of more than one coherent state. The action on the cat state,

$$|\alpha\rangle_{\mathbf{c}} \equiv \frac{[|\alpha\rangle + i|-\alpha\rangle]}{\sqrt{2}}, \tag{4}$$

is

$$\exp\left(-\frac{iFx\Delta t}{\hbar}\right)|\alpha\rangle_{\mathbf{c}} = \frac{[|\alpha + i\delta\rangle + ie^{i\theta}|-\alpha + i\delta\rangle]}{\sqrt{2}}, \tag{5}$$

where the shift in the quantum phase of the cat state is

$$\theta = 2\delta \,\mathrm{Re}[\alpha], \tag{6}$$

and we have factored out an unimportant global phase. It is important to note that the quantity we refer to here as the *quantum phase*, being the phase difference between two components of a superposition, is not (in general) the same as the *phase of the oscillator*. The latter is changed by the free evolution of the oscillator, and for the coherent state $|\alpha\rangle$ is given by the phase of the complex amplitude α. For the cat state $|\alpha\rangle_{\mathbf{c}}$ the average phase of the oscillator is undefined, since the phase distribution has peaks at $\arg(\alpha)$ and $\arg(\alpha) + \pi$.

The phase signal θ comes with a limitation not shared by the classical shift δ. Since θ appears as a phase shift between two nearly orthogonal states, it is essentially a rotation in a two-dimensional state space. Because of this, each single-shot measurement gives just 1 bit of information regarding θ. Thus while the precision of the force measurement via the cat state can be made much smaller than the classical value by using $\alpha \gg 1$, it cannot be smaller than ~ 1 (see below). Thus the quantum method will beat the classical method per shot when the force to be measured is sufficiently small that the classical single-shot error is much larger than unity, meaning that the momentum shift $\Delta p = F\Delta t \ll \sqrt{m\omega\hbar/2}$.

We note that squeezed states also provide a way to realize quantum-enhanced sensitivity at the Heisenberg limit (meaning a sensitivity that scales as the square root of the mechanical energy [33,34]). Nevertheless, cat states have a number of potential advantages over squeezed states: cat states can be prepared in a time that is independent of amplitude, the enhancement from squeezed states is limited by the degree of squeezing, and the cat-state method can be generalized to provide an additional quantum enhancement of $\sqrt{N}$ by using entangled cat states of N oscillators. It is also important to note that the (quantum-enhanced) scaling of sensitivity with phonon number that we consider here is quite distinct from that of the precision of an interferometer (in that case with a photon number). The latter scaling is often discussed in the context of force measurement [e.g., Laser Interferometer Gravitational-wave Observatory (LIGO) [21,35,36]] because interferometers are used in this context to make position measurements on mechanical oscillators. The pulsed measurement method we consider here does not use either a position measurement or an interferometer. As such, the resources involve the mechanical amplitude instead of that of the auxiliary cavity modes of interferometric schemes.

A key question when using a cat state for force metrology is how to extract that quantum phase information from the

cat state. This information cannot be extracted by a phase measurement because it does not change the phase of the oscillator. To date, one method for doing this has been proposed using an ion trap [37,38]. In this case, the internal states of the ions are used to create the initial cat state, and the phase information is then written onto the internal states of one of the ions for read-out. The scheme we present here works in quite a different way, and the required control operations are significantly simpler.

In Sec. II we show how a Kerr nonlinearity transforms the force signal imprinted on the superposition into a change in the average phase of the oscillator, and how the force can be inferred from homodyne measurements. In Sec. III we discuss an implementation of the metrology scheme using an electromechanical circuit, and in Sec. IV we analyze the functioning of this circuit including the effects of thermal noise and photon loss. In Sec. V we see how this circuit would perform if implemented with physical parameters similar to those achieved in recent experiments. Section VI concludes with some remarks on future directions.

II. SIGNAL PROCESSING WITH A KERR NONLINEARITY

We now show that a Kerr nonlinearity [39–41] can be used to translate the force signal discussed above—the phase of the superposition—into a shift of the average value of the phase of the oscillator. Conveniently, the Kerr nonlinearity will also generate cat states from initial coherent states. Let us define the two operators

$$V \equiv \exp\left(-\frac{iFx\Delta t}{\hbar}\right) = \exp(-i\delta\tilde{x}) = D(-i\delta), \tag{7}$$

$$U \equiv \exp[-i(\pi/2)(a^\dagger a)^2], \tag{8}$$

in which $\tilde{x} = a + a^\dagger$ is the dimensionless position and

$$D(\beta) = \exp(\beta a^\dagger - \beta^* a), \tag{9}$$

is the standard displacement operator. The operator V gives the action of a resonant force F for a time Δt, and the operator U gives the action of a Kerr nonlinearity for the time required to produce a cat state. Specifically, $U|\alpha\rangle = |\alpha\rangle_{\mathbf{c}}$.

To show that a Kerr nonlinearity will transform the quantum phase θ into an average phase shift of the oscillator, we apply the force to an initial cat state $|\alpha\rangle_{\mathbf{c}}$ followed by the Kerr evolution

$$U^\dagger = \exp[i(\pi/2)(a^\dagger a)^2] = \exp[-i(3\pi/2)(a^\dagger a)^2]. \tag{10}$$

We then calculate the average value of the quadrature,

$$X = \frac{\tilde{x}}{2} = \frac{a + a^\dagger}{2}, \tag{11}$$

in the resulting state. We have

$$\langle X \rangle = \frac{1}{2}(\langle \alpha|_{\mathbf{c}} V^\dagger U) X (U^\dagger V |\alpha\rangle_{\mathbf{c}})$$
$$= \mathrm{Re}\left[\langle \alpha, \theta|_{\mathbf{c}}(UaU^\dagger)|\alpha, \theta\rangle_{\mathbf{c}}\right], \tag{12}$$

in which we have defined

$$|\alpha, \theta\rangle_{\mathbf{c}} = \frac{[|\alpha + i\delta\rangle + ie^{i\theta}|-\alpha + i\delta\rangle]}{\sqrt{2}}. \tag{13}$$

Possibly the simplest way to evaluate the last line of Eq. (12) is to rewrite the operator expression $UaU^\dagger$ by noting that it is merely the operator a evolved by the Kerr nonlinearity. The equation of motion for a under the Hamiltonian $H_K = \hbar q(a^\dagger a)^2$, given by

$$\dot{a} = i[a,q(a^\dagger a)^2] = 2qi(a^\dagger a)a, \qquad (14)$$

can be solved because $a^\dagger a$ is a constant of the motion for this evolution. The result is

$$UaU^\dagger = i \exp(i\pi a^\dagger a)a \equiv iGa. \qquad (15)$$

We can now use the fact that $G|\alpha\rangle = |-\alpha\rangle$ to evaluate the last line of Eq. (12), which gives

$$\langle X \rangle = \mathrm{Re}[\langle \alpha,\theta|_{\mathbf{c}} iGa|\alpha,\theta\rangle_{\mathbf{c}}]$$
$$= e^{-2\delta^2}\{\alpha\cos(4\alpha\delta) - \delta[\sin(4\alpha\delta) - e^{-2\alpha^2}]\}. \qquad (16)$$

We see that the amplitude quadrature contains the force signal, δ. However, for a good metrology scheme, the quantity we measure should be sensitive ideally to first-order changes in the signal. We can arrange this by applying an "offset" force to apply an initial phase of $\theta_0 = -\pi/4$ prior to the action of the force F. This means applying a force that shifts the value of δ by $\delta_0 = \theta_0/(2\mathrm{Re}[\alpha]) = -\pi/(8\mathrm{Re}[\alpha])$. Note that due to the appearance in $\langle X \rangle$ of the Gaussian factor $e^{-2\delta^2}$, we want to keep $|\delta_0| \lesssim 1$, which requires that we choose $\alpha \gtrsim \pi/8 \approx 0.4$. The result is

$$\langle X \rangle = e^{-2(\delta_0+\delta)^2}\{\alpha\sin(4\alpha\delta) + \delta[\cos(4\alpha\delta) - e^{-2\alpha^2}]\}. \quad (17)$$

Restricting the size of the measured force so that $\alpha\delta \ll 1$, and allowing α to be large enough to neglect the term $e^{-2\alpha^2}$, we obtain

$$\langle X \rangle = e^{-2\delta_0^2}[\alpha(4\alpha\delta) + \delta] + \mathcal{O}[(4\alpha\delta)^2], \quad 4\alpha\delta \ll 1. \quad (18)$$

It might appear from the above expression that the average value of X is proportional to the square of α. Nevertheless, we will find that the sensitivity of the measurement is proportional to α, not α^2.

While the mean value of $\langle X \rangle$ in the processed state contains the force signal, the distribution of X is multipeaked. Using the fact that

$$U^\dagger|\alpha\rangle = [|\alpha\rangle - i|-\alpha\rangle]/\sqrt{2}, \qquad (19)$$

the processed state $|\psi\rangle = U^\dagger V U|\alpha\rangle$ is given by

$$|\psi\rangle = (|\alpha + i\delta\rangle - ie^{i\theta}|\alpha - i\delta\rangle)/2$$
$$+ i(|-\alpha + i\delta\rangle + ie^{i\theta}|-\alpha - i\delta\rangle)/2. \qquad (20)$$

As long as δ is sufficiently small, we can approximate this state by

$$|\psi\rangle \approx \left(\frac{1 - ie^{i\theta}}{2}\right)|\alpha\rangle + i\left(\frac{1 + ie^{i\theta}}{2}\right)|-\alpha\rangle$$
$$\approx \left(\frac{[1+\theta] - i}{2}\right)|\alpha\rangle + i\left(\frac{[1-\theta] + i}{2}\right)|-\alpha\rangle, \quad (21)$$

in which the last line requires $\theta \ll 1$. Since the coherent states $|\pm\alpha\rangle$ give Gaussian wave functions for the observable X, centered, respectively, at $\pm\alpha$, the distribution for X has two peaks. We see that the reason the average value of X is shifted

away from zero is that the *weights* of the two peaks are no longer equal. It is the difference in the weighting of the peaks that carries the information about the force signal θ.

As long as $\mathrm{Re}[\alpha] \gtrsim 5$, the two peaks are well separated. Upon making a measurement of X, we obtain a value greater than zero with probability $p_+ \approx (1 + \theta)/2$. Determining θ is therefore the problem of determining the probability of an unfair coin. We also see that one of the factors of α in the expression for $\langle X \rangle$ is merely due to the placing of the peaks of the distribution at $\pm\alpha$. This is irrelevant to the determination of the probability p_+, however, which is why the sensitivity scales as α even though $\langle X \rangle$ is proportional to α^2.

To determine p_+, we make M measurements of X, and the resulting estimate for δ is calculated from

$$S = \frac{m}{M} - \frac{1}{2} = 2\alpha\left[1 - \frac{1}{(2\alpha)^2}\right]\delta, \qquad (22)$$

in which m is the number of times we obtain the result $X > 0$. The error in S is due to the fluctuations of m/M, whose standard deviation for large m is

$$\sigma = \sqrt{\frac{(1/2 + S)(1/2 - S)}{M}} = \frac{1}{2\sqrt{M}} \qquad (23)$$

as long as $S \ll 1$.

Two additional properties of the above scheme are worth noting. The first is the way in which the force appears in the phase shift, $4\alpha\delta$. Since this phase shift is proportional to $\mathrm{Re}[\alpha]$, and complex number α rotates at the mechanical frequency, the detection scheme filters the force signal: a constant force produces no signal if it acts for an integral number of periods, whereas the shift produced by a force at the mechanical frequency simply grows with time. The scheme thus filters the force in a band around the mechanical frequency, where the bandwidth is inversely proportional to the time the state spends in the mechanics. This filter is also nonlinear. The second property is that the filter is phase-selective: because the phase shift is proportional to the real part of α, it primarily detects the quadrature that is in phase with the resonator. To measure both quadratures, one could either use two devices or shift the phase of the mechanical oscillator periodically.

III. CIRCUIT IMPLEMENTATION

A. Unidirectional coupling via an isolator

To implement the metrology procedure described above, we need to somehow prepare a mechanical resonator in a cat state. To prepare such a state requires a nonlinear device, and thus something other than the mechanical resonator itself. The approach we take is to use a nonlinear (Josephson) electrical oscillator to prepare the state and then transfer it to the mechanical oscillator. Implementing such a transfer requires coupling the mechanical oscillator to an "auxiliary" electrical oscillator with a very large photon number. This high amplitude is required to achieve a sufficiently strong coupling with the mechanics. There is a catch, however: directly coupling a nonlinear oscillator to the linear auxiliary (so as to pass the cat state to the latter) necessarily imbues the auxiliary with some nonlinearity. This nonlinearity in turn
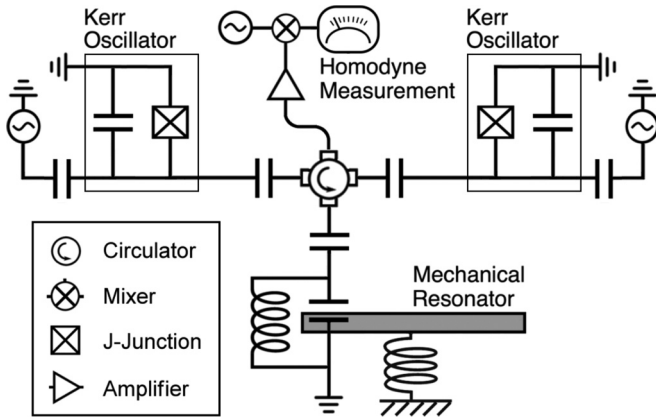
FIG. 1. An electromechanical circuit diagram that shows the layout of the component systems required to make a quantum-enhanced measurement of a force using a "cat" state. To implement such a measurement requires that the coupling between the component systems be turned off and on in a specified sequence. For simplicity, we have not explicitly included in the circuit the means by which this coupling is controlled. In the text, we describe four ways in which this can be achieved.

prevents the drive signal from preparing the auxiliary in a high amplitude state.

Our solution is to couple the nonlinear oscillator to the linear oscillator via a transmission line that includes a circulator. This effectively decouples the circuits of the two oscillators electrically while allowing a (one-way) transfer of energy via a traveling wave from the nonlinear oscillator to the auxiliary. To process the signal that is picked up by the mechanics, we must again pass the state to a nonlinear electrical oscillator. To do this, we couple the mechanical oscillator to a second linear oscillator, and we couple this oscillator to a second nonlinear oscillator via a second transmission line. This time the direction of the circulator is chosen to transfer the state from the second auxiliary to the second nonlinear oscillator. The resulting superconducting electromechanical circuit is shown in Fig. 1. We achieve the one-way connections by attaching all the components to a single circulator.

B. Implementing "pulsed" control

To implement the metrology procedure with the above circuit, we first create a cat state in the nonlinear oscillator on the left hand side in Fig. 1, which is composed of a Josephson junction in parallel with an inductor [41–43]. Creating this cat state involves driving the oscillator to prepare a coherent state with moderate amplitude in a time short compared to that of the Kerr nonlinearity, and then waiting the requisite time to allow this nonlinearity to create the cat state. The cat state must then be transferred to the mechanical oscillator in which it spends some time, and then to the nonlinear oscillator on the right in Fig. 1 via the second transmission line. The state is then processed by being left in this nonlinear oscillator for the required time, and it is subsequently transferred back to the transmission line to propagate to a homodyne measurement apparatus.

The operation of the circuit that we have just described involves a time-dependent or "pulsed" operation in which the cat state is transferred between the various component systems at specified times. In Fig. 1 we have not, however, explicitly included in the circuit the means to accomplish this control; as displayed, the coupling between the component systems is fixed. To implement the pulsed operation, we must have a way to effectively turn the coupling on and off between the components. We now describe four ways in which this could be done.

(1) Parametric circulator. It was discovered fairly recently that circulators and other nonreciprocal devices can be realized with simple networks of linear oscillators [44,45]. By giving the oscillators in the network different frequencies, and coupling them using "parametric" driving, one is able to turn the resulting pairwise couplings on and off and control the functioning of the circulator. This could be used to control which circuit elements are connected by the circulator, and it would have the added advantage that the direction of the circulation could be reversed, allowing the use of a single Kerr circuit for both preparation and readout.

(2) Tunable Kerr oscillator. If we replace the Josephson junctions in the Kerr oscillators with SQuID loops, the frequencies of these oscillators can be controlled by changing the flux through the loops. One can then tune the Kerr circuits in and out of resonance with the linear oscillator to effectively control the coupling.

(3) Tunable electromechanical circuit. We can tune the electromechanical part of the circuit (the mechanical oscillator and linear superconducting oscillator to which it is coupled) in and out of resonance with the Kerr circuits by applying a dc voltage to the drum capacitor. In this way, we can effectively change the coupling between these elements [46,47].

(4) Indirectly couple the Kerr oscillators. One way to control the coupling between the Kerr oscillators and their respective transmission lines is to couple them to these lines indirectly. To do this, one couples each Kerr oscillator to a linear oscillator, which is then coupled to the transmission line. One can then turn the coupling on and off between the Kerr oscillator and its linear oscillator by using a parametric drive. By having the linear oscillator strongly coupled to a line, this oscillator allows a rapid transfer between the Kerr oscillator and the line when the coupling is turned on [48].

IV. CIRCUIT PERFORMANCE IN THE PRESENCE OF NOISE AND LOSS

We now analyze the functioning of the circuit in Fig. 1, with the primary purpose of examining the effects of thermal noise in the mechanical oscillator and photon loss (damping) in the superconducting components. It turns out that, with a single simplification, it is possible to derive analytic expressions for the behavior of the circuit in the regime in which the number of photons lost from the Kerr oscillators remains small. The simplification involves treating the transfer of the state between each of the nonlinear oscillators and the mechanics as the action of a state-swapping interaction given by

$$H_I = i\hbar g(a^\dagger b - b^\dagger a), \tag{24}$$

in which a and b are, respectively, the annihilation operators for one of the Kerr oscillators and the mechanical mode. In fact, this simplification does not modify the process in any fundamental way. Since the transfer process is linear (and passive), no matter how exactly the time evolution of the transfer proceeds, the result is a transformation of the form

$$b(t) = c_1 a(0) + c_2 b(0) \qquad (25)$$

after some time t, in which c_1 and c_2 are complex numbers. A complete transfer from a to b means that $c_2 = 0$. If the process involves loss, then $|c_2|^2 + |c_1|^2 < 1$, and we can model this loss by including an additional mode c that absorbs the lost energy. Making the assumption that the transfer is due to the Hamiltonian H_I merely fixes the precise manner in which the coefficients $c_j(t)$ change with time. This Hamiltonian produces a sinusoidal evolution for the coefficients, and it provides an example that elucidates how the measurement result depends on this evolution and the force signal.

For purposes of theoretical analysis, we can combine the first and second nonlinear oscillators into a single oscillator that prepares the initial cat state and receives the state back from the mechanics. We can therefore break the metrology process into three parts: (i) The cat state is created in the nonlinear resonator. During this step, the state is subject to damping, so we need to examine the dynamical creation process. (Note that we do not need to explicitly consider the damping that acts during the creation of the initial coherent state in the nonlinear oscillator because this damping effects only the final coherent amplitude of this state.) (ii) The cat state is transferred into and back out of the mechanics via the action of the linear interaction H_I. During this process, the state is subject to loss in the transmission line that acts as additional damping. While the state resides in the mechanics, it is acted on by the force as well as any thermal noise to which the mechanics is subjected. The mechanical damping is much smaller than the electrical damping, and we ignore it. (iii) The state now resides back in the nonlinear oscillator and is acted upon by the Kerr evolution as well as the damping of the oscillator. At the end of step (iii), the nonlinear oscillator contains the cat state in which the force signal is encoded in the amplitude difference between the two components of the cat state, and which is measured with homodyne detection.

A. Evolution of the Kerr oscillator

When damping is included, the evolution of the nonlinear oscillator can no longer be solved analytically. Nevertheless, it is possible to obtain an analytical solution when only a small number of photons are lost during the evolution. The Hamiltonian of the Kerr oscillator is

$$H_K = \hbar \omega a^\dagger a + \hbar \mu (a^\dagger a)^2, \qquad (26)$$

where μ is the rate (or "frequency") of the nonlinearity. We will work in the interaction picture with respect to the linear oscillation at frequency ω, so that the Hamiltonian is effectively

$$H_{KI} = \hbar \mu (a^\dagger a)^2. \qquad (27)$$

When we include damping of the oscillator at the rate κ, the full evolution is given by the master equation

$$\dot{\rho} = -\frac{i}{\hbar}[H_K, \rho] - \frac{\kappa}{2}(a^\dagger a \rho + \rho a^\dagger a - 2a\rho a^\dagger). \qquad (28)$$

Most readers will probably be familiar with the "quantum jump" description of a Lindblad master equation, in which the evolution is described in terms of individual "trajectories" in which photon emissions (the "jumps") happen at a sequence of randomly sampled times. Fewer will be familiar with the version of this trajectory description in which the (stochastic) evolution equation for the trajectories is linear. Such "linear quantum trajectories" are obtained by fixing the average rate of photon emissions at κ, and omitting to normalize the state following each emission. The normalization (specifically, the square modulus) of the evolving state then furnishes the missing information regarding the probability with which a given sequence of emission times (a given trajectory) will actually occur, since by fixing the emission rate one does not sample the trajectories with the correct probabilities.

Using the linear formulation of quantum-jump trajectories, we can break the evolution up into classes of trajectories defined by the number of emissions that occur. For the present system, the evolution of each class can be solved analytically, although the complexity of the solutions increases with the number of emissions. When there are no emissions, the evolution is given by replacing the Hamiltonian with

$$H_{eff} = \hbar \mu (a^\dagger a)^2 - \hbar \frac{\kappa}{2} a^\dagger a, \qquad (29)$$

and the probability with which this evolution occurs is merely the square norm of the state at time t. Note that if we define

$$W(t) \equiv \exp(-[i/\hbar]H_{eff}t), \qquad (30)$$

then

$$W(\tau) = UY, \qquad (31)$$

where $\tau = \pi/(2\mu)$ and we have defined

$$Y = e^{-(\kappa\tau/2)a^\dagger a}. \qquad (32)$$

When there is a single photon emission at a time s during the evolution, the state at time t is

$$|\tilde{\psi}_s(t)\rangle = W(t-s)aW(s)|\psi(0)\rangle. \qquad (33)$$

Note that the state at time t is now parametrized by s. The probability density $P(s)$ that the state is $|\tilde{\psi}_s(t)\rangle$ at time t is the probability per unit time that an emission occurs under the fixed emission rate κ, multiplied by the square norm of $|\tilde{\psi}_s(t)\rangle$. The total probability for a single emission during the interval $[0,t]$ is thus

$$p_1(t) = \kappa \int_0^t |\langle \tilde{\psi}_s(t)|\tilde{\psi}_s(t)\rangle|^2 ds. \qquad (34)$$

We can now calculate the state that is prepared by the nonlinear oscillator for the cases in which 0 and 1 photons are emitted during this preparation. When no photons are lost, we use the fact that

$$e^{-i(\kappa t/2)a^\dagger a}|\alpha\rangle = \xi|\eta\alpha\rangle \qquad (35)$$

with

$$\xi = \exp\left(\frac{[\eta^2 - 1]}{2}e^{|\alpha|^2/2}\right),$$

$$\eta = e^{-\kappa\tau/2}, \tag{36}$$

to obtain

$$W(t)|\alpha\rangle = \xi\left[\frac{|\eta\alpha\rangle + i|-\eta\alpha\rangle}{\sqrt{2}}\right] = \xi|\eta\alpha\rangle_{\mathbf{c}}. \tag{37}$$

To calculate the final state when there is a photon emission at time $0 \leqslant s \leqslant \tau$, we first swap the operator a through $W(s)$ to obtain

$$W(\tau - s)aW(s) = -i\eta UY^2 e^{-i\mu s a^\dagger a}a. \tag{38}$$

The state at time τ, given a photon emission at time s, is thus

$$|\psi_1\rangle = -i\eta\alpha\xi\left[\frac{|\eta^2\alpha e^{-i\phi}\rangle - i|\eta^2\alpha e^{-i\phi}\rangle}{\sqrt{2}}\right], \tag{39}$$

where the angle through which the coherent states are rotated is $\phi = \mu s$ so that

$$0 \leqslant \phi \leqslant \pi. \tag{40}$$

Under the assumption that $\kappa\tau \ll 1$, the distribution of emission times s, and thus the distribution of ϕ in the interval $[0,\pi]$, is approximately uniform. We see that a photon emission during the preparation of the cat state rotates the cat state by a random phase up to $180°$. This is very useful information, and we will return to it later.

B. Swapping through the mechanical oscillator

In the second part of the process, the cat state is swapped into the mechanical oscillator and back into the nonlinear oscillator. We assume that either (i) the swap is fast compared to the nonlinearity so that the evolution is effectively linear during the swap, or (ii) the nonlinearity is tunable and can be reduced effectively to zero during the swap. With these assumptions, the evolution during the swapping operation is linear, and because of this we can obtain a complete solution including damping and thermal noise for the mechanical oscillator.

As explained above, we model the dynamics of the swap operation using the linear interaction Hamiltonian H_I given in Eq. (24). Since the frequency of the nonlinear oscillator, Ω, is much higher than that of the mechanical oscillator, ω, the interaction between the auxiliary and the latter must be modulated (by modulating the drive on the auxiliary [41,49]) at the frequency difference between them. With this modulation, and using the rotating-wave approximation, in the interaction picture with respect to the Hamiltonian

$$H_0 = \hbar\Omega a^\dagger a + \hbar\omega b^\dagger b \tag{41}$$

the Hamiltonian of the two-oscillator system becomes

$$H = i\hbar g(a^\dagger b - b^\dagger a). \tag{42}$$

Including damping and thermal noise, the full evolution of the two oscillators is given by the quantum Langevin equations of the input-output formalism as [41,50]

$$\dot{a} = -(\tilde{\kappa}/2)a + gb + \sqrt{\tilde{\kappa}}a_{\text{in}}(t), \tag{43}$$

$$\dot{b} = -(\gamma/2)b - ga + \sqrt{\gamma}b_{\text{in}}(t) + e^{i\omega t}f(t) + \mathcal{T}(t). \tag{44}$$

Here $\tilde{\kappa}$ models the combined damping coming from the nonlinear oscillator, the auxiliary, and the transmission line, γ is the damping rate of the mechanics, and a_{in} and b_{in} are the quantum (vacuum) noise from the respective environments to which the oscillators damp. The dimensionless version of the force to be measured is $f(t)$, which in terms of the real force F is

$$f(t) = F(t)\sqrt{\frac{2}{m\hbar\omega}}. \tag{45}$$

We have split off the thermal component of the noise from the input field b_{in} so that $\mathcal{T}(t)$ is a classical white noise describing the thermal fluctuations from the environment [51]. The various noise sources are described by the correlation functions

$$\langle a_{\text{in}}(t)a_{\text{in}}(t')\rangle = \langle b_{\text{in}}(t)b_{\text{in}}(t')\rangle = \delta(t' - t), \tag{46}$$

$$\langle\mathcal{T}(t)\mathcal{T}(t')\rangle = [2n_T(\Omega) + 1]\delta(t' - t), \tag{47}$$

in which $n_T(\Omega)$ is the average thermal occupation number of an oscillator with frequency Ω at the temperature of the environment, namely

$$n_T(\Omega) = \left[\exp\left(\frac{k_B T_{\text{env}}}{\hbar\omega}\right) - 1\right]^{-1}, \tag{48}$$

in which T_{env} is the temperature and k_B is Boltzmann's constant.

Solving the above linear equations of motion, using standard methods, one obtains

$$\begin{pmatrix}a(t)\\b(t)\end{pmatrix} = M(t)\begin{pmatrix}a(0)\\b(0)\end{pmatrix} + \begin{pmatrix}A_{\text{in}}(t) + i\delta'\\B_{\text{in}}(t)\end{pmatrix}, \tag{49}$$

where

$$M = e^{-\Gamma t}\begin{pmatrix}\cos(\nu t) & -i\sin(\nu t)e^{i\psi}\\-i\sin(\nu t)e^{-i\psi} & \cos(\nu t)\end{pmatrix} \tag{50}$$

and

$$\Gamma = \frac{\gamma + \tilde{\kappa}}{4}, \tag{51}$$

$$q \equiv \frac{\gamma - \tilde{\kappa}}{4g}, \tag{52}$$

$$\nu = g\sqrt{1 - q^2}, \tag{53}$$

$$\psi = \arg\left[q + i\sqrt{1 - q^2}\right]. \tag{54}$$

The driving terms produce the additional "displacements" $A_{\text{in}}(t)$, $B_{\text{in}}(t)$, and δ'. The first two represent integrals over the input vacuum fields, and the third is an integral over the classical drives, which are the force and the thermal noise. We will find that we do not need the first two since they will vanish in the expectation value that we need to calculate. The third

term is given by

$$\delta' = \text{Re}\left\{ \int_0^{\pi/\nu} \sin(\nu s) e^{i\omega s} [f(s) + \mathcal{T}(s)] \, ds \right\}, \quad (55)$$

which contains the force signal $f(t)$ and the thermal noise $\mathcal{T}(t)$.

A complete swap to and from the mechanical resonator is achieved at time $T = \pi/\nu$ (or integer multiples thereof), at which point we have

$$a(T) = e^{-\Gamma T} a(0) + A_{\text{in}}(T) + i\delta'. \quad (56)$$

The fact that the magnitude of the coefficient of $a(0)$ in the above equation is less than unity implies that energy has been lost from the system to the vacuum modes. We can simplify the calculation of the signal in the next section by introducing a unitary operator that generates the transformation $a(0) \to a(T)$. To do this, we must introduce an additional (fictitious) mode or modes that receive the energy lost from the nonlinear oscillator. Using a single mode, and denoting the annihilation operator for this mode by c, we note that if we define

$$L = \exp(r a^\dagger c - r c^\dagger a) D(-i\delta'), \quad (57)$$

then

$$L^\dagger a(0) L = \cos(r) a(0) + \sin(r) c(0) + i\delta'. \quad (58)$$

By choosing r to satisfy $\cos r = e^{-\Gamma T}$, we see that the transformation generated by L is the same as that in Eq. (56) except for the fact that we have replaced the vacuum field A_{in} with the single vacuum mode c. Since neither of these terms contributes to the signal, this difference is not important.

C. Calculating the signal

Now that we have captured the dynamics of the process in terms of relatively simple operators W and L, calculating the signal is feasible. We first calculate the signal given that no photons are lost during the process. The initial state of the Kerr oscillator is $|\alpha\rangle$ and that of the fictitious auxiliary we introduced above is the vacuum. The initial state of the resonator can be omitted since it plays no role in the signal. Writing the initial joint state as $|\alpha\rangle|0\rangle$, when no photons are lost the expression for $\langle X \rangle$ is

$$\langle X \rangle_0 = \mathcal{N}^{-1} \text{Re}[\langle 0|\langle \alpha| W^\dagger L^\dagger W a W^\dagger L W |\alpha\rangle|0\rangle] \quad (59)$$

in which $\mathcal{N}$ is the normalization discussed above, and it is given by

$$\mathcal{N} = \langle 0|\langle \alpha| W^\dagger L^\dagger W W^\dagger L W |\alpha\rangle|0\rangle. \quad (60)$$

The apparent simplicity of the expressions in Eqs. (59) and (60) is somewhat deceptive: it is considerably more challenging to evaluate than Eq. (16). We proceed by first applying LW to the state $|\alpha\rangle$. Using Eqs. (37) and (57), and defining

$$|\beta, \tilde{\theta}, q\rangle \equiv \frac{|\beta + q\rangle + i e^{i\tilde{\theta}}|-\beta + q\rangle}{\sqrt{2}}, \quad (61)$$

we have

$$LW|\alpha\rangle = \xi |z\eta\alpha, \tilde{\theta}, -iz\delta'\rangle \quad (62)$$

with

$$z = \cos(r) = e^{-\Gamma T}, \quad (63)$$

$$\tilde{\theta} = 2\eta\delta'\text{Re}[\alpha]. \quad (64)$$

To complete the calculation of $\mathcal{N}$ and $\langle X \rangle_0$, we need to calculate the expectation values of the operators

$$W W^\dagger = e^{-\kappa t a^\dagger a}, \quad (65)$$

$$W a W^\dagger = i e^{-\kappa t a^\dagger a} a e^{-i\pi a^\dagger a} \quad (66)$$

for the state on the right-hand side of Eq. (62). Since these operators change the amplitude and normalization of coherent states, but otherwise preserve their coherent-state nature, calculating these expectation values finally reduces to calculating four inner products between various coherent states. Using the relation

$$\langle \alpha|\beta\rangle = \exp\left(-\frac{|\alpha|^2 + |\beta|^2}{2} + \alpha^*\beta \right), \quad (67)$$

a rather lengthy calculation gives

$$\begin{aligned} \mathcal{N}\langle X \rangle_0 &= \eta \exp(-\epsilon_+|\tilde{\delta}|^2) \exp(-\epsilon_- \eta^2 \alpha^2) \\ &\quad \times [\eta z \alpha \sin(2\epsilon_+ \eta\alpha \, \text{Re}[\delta']) \\ &\quad + \text{Re}[\tilde{\delta}] \cos(2\epsilon_+ \eta\alpha \, \text{Re}[\delta'])], \quad (68) \\ &\quad + \eta \exp(-(1 + \eta^4)(\eta^2\alpha^2 + |\tilde{\delta}|^2)) z \, \text{Re}[\tilde{\delta}] \\ &\quad \times \cosh(2[1 + \eta^4]\eta\alpha \, \text{Im}[\tilde{\delta}]), \quad (69) \end{aligned}$$

where the normalization is

$$\begin{aligned} \mathcal{N} &= \exp(-\epsilon_-|\tilde{\delta}|^2)[\exp(-\epsilon_- \eta^2\alpha^2) \cosh(2\epsilon_- \eta\alpha \, \text{Im}[\tilde{\delta}]) \\ &\quad + \exp(-\epsilon_+ \eta^2\alpha^2) \cos(2\epsilon_- \eta\alpha \, \text{Re}[\delta'])]. \quad (70) \end{aligned}$$

Here we have defined $\epsilon_\pm \equiv (1 \pm \eta^2)$ and the force-induced shift

$$\tilde{\delta} = \delta_0' + \delta', \quad (71)$$

where $\delta_0' = \pi/(4\epsilon_+ \eta\alpha)$ is the offset shift required to provide the optimal offset phase $\theta_0 = -\pi/4$, as discussed in Sec. II.

Naturally we wish to operate the device in the regime in which the probability of photon loss is low. Making the approximation that

$$\gamma\tau \lesssim \kappa\tau \ll 1, \quad (72)$$

we have

$$\eta \approx 1 - \kappa\tau/2, \quad (73)$$

$$\epsilon_+ \approx 2\eta, \quad (74)$$

$$\epsilon_- \approx \kappa\tau, \quad (75)$$

which gives the considerably simpler expression

$$\langle X \rangle_0 = \eta e^{-2\eta|\delta'|^2 - \kappa\tau\alpha^2} [z\eta\alpha \sin(4\eta^2\alpha\delta') + \delta' \cos(4\eta^2\alpha\delta')]$$

in which $z = e^{-\Gamma T}$. We have also dropped the part of $\langle X \rangle_0$ that is suppressed by the factor $e^{-2\alpha^2}$ under the assumption that

$\alpha \gg 1$. Assuming in addition that $\alpha\delta' \ll 1$, we obtain

$$\langle X \rangle_0 = z\eta^2\alpha(4\eta^2\alpha\delta') + \eta\delta'. \quad (76)$$

Having calculated the signal when no photons are lost from the system during the nonlinear processes, we must now examine what happens when a photon is lost. Note that the linear part of the evolution, that in which the state is swapped though the mechanical oscillator, already takes into account photon loss, so it is only when photons are lost during the nonlinear evolution that we must now consider. We examined this case in Sec. IV A, where we found that a single photon emission during the evolution in the Kerr oscillator rotates the cat state in phase space by a random phase, approximately uniformly distributed between zero and π. For a uniform random phase, the average signal is zero. Recall that the way we obtain the force from the signal is to perform the process multiple times, and the force is given by the number of times the value of the signal is greater than zero. Specifically, it is the imbalance between the frequencies of obtaining a positive and negative signal. When a photon (and thus when any number of photons) is lost during the process, these frequencies are equalized, thus reducing the imbalance for a given force. Thus if we know the probability that one or more photons will be lost, we can obtain the formula for the force merely by correcting for the reduction in the imbalance. The effect of photons on the accuracy of the estimate is merely that the fractional error in S increases (for a given number of repetitions) purely because the average value of S is reduced.

Denoting the probability that one or more photons are lost by P, the new formula for S is

$$S = \frac{1}{2} - \frac{m}{M} = 2\alpha'\left[1 + \frac{\eta e^{\Gamma T}}{(2\alpha')^2}\right](1 - P)\delta', \quad (77)$$

in which

$$\alpha' \equiv \eta^2\alpha = e^{-\kappa\tau}\alpha, \quad (78)$$

$$P = \pi\kappa\alpha^2/\mu. \quad (79)$$

A key result of the above analysis is that (i) single-photon emissions all but destroy the information in the measurement result, but (ii) since multiple repetitions of the measurement are required to obtain an accurate result, such emissions do not significantly effect the measurement process as long as the probability of an emission per shot, P, is much less than unity. The effect of emissions is to reduce the quantum advantage from a scaling of α to one of α'.

Making the approximations in Eqs. (72)–(75) to simplify the form of $\langle X \rangle_0$ is useful to gain insight, but we may want to use the full expression when determining the force from the signal. For the purposes of examining deviations from the simplified formula, it is useful to write S in terms of $\langle X \rangle_0$, which is

$$S = \frac{1}{2} - \frac{m}{M} = \left(\frac{(1 - P)}{z\eta^2\alpha}\right)\langle X \rangle_0. \quad (80)$$

We now return to the question of the time dependence of the transfer of the state between the oscillators. As explained above, we assumed in our calculation that this transfer was implemented by an interaction of the form given in Eq. (24).

During the transfer, if we think of the state as being "partially" in the mechanical resonator, then the interaction we have chosen fixes the way in which the amount of the state in this resonator changes with time. Calculating the expectation value of $\langle X \rangle$ with a specific form for this time evolution allows us to see how the result will change if the time evolution of the swap is modified. In general, since we are using a transmission line to implement the state transfer, the time dependence will depend on the exact protocol used. (The protocol involves effectively turning the coupling on and off between each oscillator and the transmission line to effect the transfer, and the time dependence of the transfer is determined by the time dependence chosen for the couplings.)

We see from the form of the signal δ' that the time-dependent envelope of the transfer, which is sinusoidal in our treatment, appears in the time integral that gives the overall phase generated by the force. This is easily understood: if only a fraction of the state is contained in the mechanical oscillator at a given time, then we would expect the effect of the force to be similarly reduced. Thus the effect of changing the time envelope of the transfer will be to change the envelope functions that appear in the integral for the accumulated phase shift δ', and possibly to modify slightly the relative contributions of the damping rates κ and γ to the overall photon loss.

V. IMPLEMENTATION WITH THE PRESENT TECHNOLOGY

We now consider the experimental parameters required to realize the above scheme, while keeping the loss probability P small. The primary requirement is that the Kerr rate μ should be large compared to the photon emission rates $\alpha^2\kappa$ and $\alpha^2\gamma$. In recent experiments [27], typical values that have been achieved for the mechanical oscillator are $\omega/2\pi = 10$ MHz with $\gamma/2\pi = 10$ Hz and an ambient temperature giving $\tilde{n} = 50$. Linear electrical resonators have frequencies of 5–10 GHz and damping rates around $\kappa/2\pi = 100$ kHz. As discussed above, in the absence of an oscillator whose nonlinearity can be tuned over a sufficiently large range, we employ a transmission line to couple the Kerr oscillators to the mechanics. The transfer rate, or effective coupling rate g, is then limited by the rate at which the oscillators damp to the transmission lines. A rate of $g/2\pi = 500$ kHz is certainly achievable [26,30]. The Kerr nonlinearity can be made quite large ($\mu \sim 50$ MHz) without difficulty, but it brings with it an increased loss rate, κ. Since γ is typically much less that κ, it is the ratio of μ to κ that is the key factor that limits the implementation.

To achieve a single-photon loss probability equal to P, we need the ratio of μ to κ to be

$$\frac{\mu}{\kappa} = \frac{\pi\alpha^2}{P}, \quad (81)$$

in which α^2 is the average number of photons in the resonator. Thus to achieve $P \leqslant 10\%$ for $\alpha = 1.5$ requires $\mu/\kappa \approx 70$. This would be satisfied, for example, by an oscillator with the pair of parameters $\mu/2\pi = 7$ MHz and $\kappa/2\pi = 100$ kHz. With a transfer rate $g/2\pi = 500$ kHz, the loss factors $\gamma\tau$ and $\kappa\tau$ are approximately 10^{-4} and 0.2, respectively, using the loss rates presented above. This collection of parameters would,
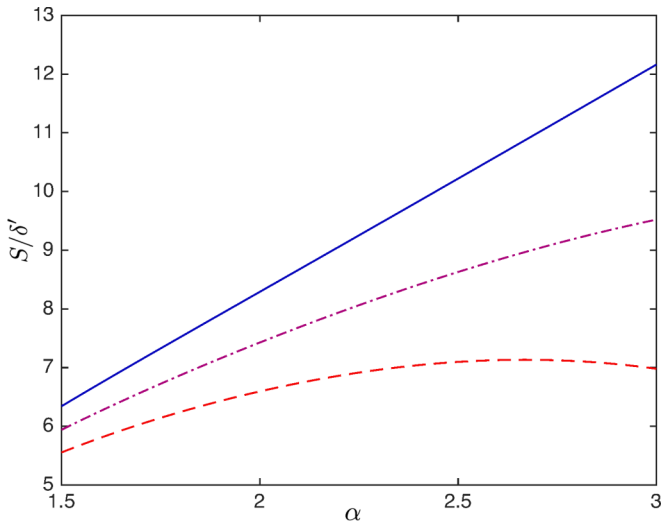
FIG. 2. Here we show the performance of a quantum nano-electromechanical circuit designed to make a quantum-enhanced measurement of a force (an accelerometer) in the presence of photon loss. The y axis is the (dimensionless) measured signal, S [given by Eq. (80)], divided by a quantity δ' [Eq. (55)] that is essentially a filtered version of the force (including any thermal noise). The dark (blue) plot gives the ideal performance when there is no photon loss, and it displays the linear dependence on the amplitude of the superposition state, α, which is the distinct quantum effect. The physical parameters are those given in Sec. V, but with no loss ($\kappa = \gamma = 0$). The dash-dotted (mauve) curve is for the same parameters but with a loss rate of $\mu/\kappa = 140$ [$\kappa/(2\pi) = 50$ kHz $= 500\gamma$]. The dashed curve has the same values for the parameters as the dash-dotted curve, except that κ is increased by a factor of 2.

therefore, allow one to demonstrate an increase of the force signal as a function of α, being the signature of the uniquely quantum effect. In Fig. 2 we show the signal as a function of α for the physical parameters described above, and for three values of the photon loss rate κ with $\kappa' = \kappa$. For these plots, we use the full expression for the signal S given by Eq. (80).

VI. CONCLUDING REMARKS

A superposition of coherent states, often referred to as a "Schrödinger cat," can be used to measure a linear force in a way that scales with the amplitude of the probe oscillator. We have presented a quantum electromechanical circuit that could potentially be used to realize this measurement. The operation of the circuit involves repeating a process in which a cat state is produced, swapped into and back out of a mechanical resonator, and then processed by a Kerr nonlinearity so that the signal can be read out using a homodyne measurement. Each time the process is repeated, the measurement provides a binary result, and the relative frequency of the two outcomes gives the estimate of the force.

The cat state is sensitive to an applied force because the force induces a shift in the phase between the complex amplitudes of the two components of the superposition. But this signal is a phase shift in an effectively two-dimensional Hilbert space, and it is for this reason that each repetition of the measurement procedure provides no more than 1 bit of information about the force. Thus while the use of cat states can lead to increased sensitivity, many repetitions are required to obtain high accuracy. This begs the question of whether there might be other quantum states that are able to provide more information (resolution) per measurement, and ideally for which this resolution increases with the amplitude. In fact, this question has recently been answered in the affirmative by Duivenvoorden *et al.*, who have called the state in question a "grid" state. A natural direction for further work is to explore the space of states with these properties, and to find even simpler ways in which these states can be used for accelerometry. In metrology, the simplicity of the process is important in reducing the number of physical parameters that must be controlled in order to realize the potential gains in precision. While our primary motivation was to present a relatively simple way to perform quantum-enhanced accelerometry, we expect that our scheme still leaves considerable room for improvement—at least, it seems that simpler schemes should exist. The search for schemes with increasing simplicity, and thus practicality, is an important direction for future work.

[1] V. Giovannetti, S. Lloyd, and L. Maccone, Science **306**, 1330 (2004).

[2] J. P. Dowling, Contemp. Phys. **49**, 125 (2008).

[3] V. Giovannetti, S. Lloyd, and L. Maccone, Nat. Photon. **5**, 222 (2011).

[4] M. A. Taylor and W. P. Bowen, Phys. Rep. **615**, 1 (2016).

[5] J. N. Gannaway and C. J. R. Sheppard, Opt. Quantum Electron. **10**, 435 (1978).

[6] C. M. Caves, Phys. Rev. D **23**, 1693 (1981).

[7] J. J. Bollinger, W. M. Itano, D. J. Wineland, and D. J. Heinzen, Phys. Rev. A **54**, R4649(R) (1996).

[8] S. F. Huelga, C. Macchiavello, T. Pellizzari, A. K. Ekert, M. B. Plenio, and J. I. Cirac, Phys. Rev. Lett. **79**, 3865 (1997).

[9] N. Treps, U. Andersen, B. Buchler, P. K. Lam, A. Maître, H.-A. Bachor, and C. Fabre, Phys. Rev. Lett. **88**, 203601 (2002).

[10] P. Kok, S. L. Braunstein, and J. P. Dowling, J. Opt. B **6**, S811 (2004).

[11] V. Giovannetti, S. Lloyd, and L. Maccone, Phys. Rev. Lett. **96**, 010401 (2006).

[12] B. L. Higgins, D. W. Berry, S. D. Bartlett, H. M. Wiseman, and G. J. Pryde, Nature (London) **450**, 393 (2007).

[13] S. Boixo, A. Datta, M. J. Davis, S. T. Flammia, A. Shaji, and C. M. Caves, Phys. Rev. Lett. **101**, 040403 (2008).

[14] D. W. Berry, B. L. Higgins, S. D. Bartlett, M. W. Mitchell, G. J. Pryde, and H. M. Wiseman, Phys. Rev. A **80**, 052114 (2009).

[15] S. Gröblacher, K. Hammerer, M. R. Vanner, and M. Aspelmeyer, Nature (London) **460**, 724 (2009).

[16] W. Wasilewski, K. Jensen, H. Krauter, J. J. Renema, M. V. Balabas, and E. S. Polzik, Phys. Rev. Lett. **104**, 133601 (2010).

[17] M. H. Schleier-Smith, I. D. Leroux, and V. Vuletić, Phys. Rev. A **81**, 021804 (2010).

[18] M. Tsang and C. M. Caves, Phys. Rev. Lett. **105**, 123601 (2010).

[19] H. Zhang, R. McConnell, S. Ćuk, Q. Lin, M. H. Schleier-Smith, I. D. Leroux, and V. Vuletić, Phys. Rev. Lett. **109**, 133603 (2012).

[20] E. Verhagen, S. Deleglise, S. Weis, A. Schliesser, and T. J. Kippenberg, Nature (London) **482**, 63 (2012).

[21] J. Aasi, J. Abadie, B. P. Abbott, R. Abbott, T. D. Abbott, M. R. Abernathy, C. Adams, T. Adams, P. Addesso *et al.*, Nat. Photon. **7**, 613 (2013).

[22] M. J. Woolley and A. A. Clerk, Phys. Rev. A **87**, 063846 (2013).

[23] J. G. Bohnet, K. C. Cox, M. A. Norcia, J. M. Weiner, Z. Chen, and J. K. Thompson, Nat. Photon. **8**, 731 (2014).

[24] P. Komar, E. M. Kessler, M. Bishof, L. Jiang, A. S. Sorensen, J. Ye, and M. D. Lukin, Nat. Phys. **10**, 582 (2014).

[25] K. Jacobs, N. Tezak, H. Mabuchi, and R. Balu, J. Opt. **18**, 034002 (2016).

[26] J. D. Teufel, D. Li, M. S. Allman, K. Cicak, A. J. Sirois, J. D. Whittaker, and R. W. Simmonds, Nature (London) **471**, 204 (2011).

[27] J. D. Teufel, T. Donner, D. Li, J. W. Harlow, M. S. Allman, K. Cicak, A. J. Sirois, J. D. Whittaker, K. W. Lehnert, and R. W. Simmonds, Nature (London) **475**, 359 (2011).

[28] T. A. Palomaki, J. W. Harlow, J. D. Teufel, R. W. Simmonds, and K. W. Lehnert, Nature (London) **495**, 210 (2013).

[29] T. A. Palomaki, J. D. Teufel, R. W. Simmonds, and K. W. Lehnert, Science **342**, 710 (2013).

[30] F. Lecocq, J. D. Teufel, J. Aumentado, and R. W. Simmonds, Nat. Phys. **11**, 635 (2015).

[31] G. Kirchmair, B. Vlastakis, Z. Leghtas, S. E. Nigg, H. Paik, E. Ginossar, M. Mirrahimi, L. Frunzio, S. M. Girvin, and R. J. Schoelkopf, Nature (London) **495**, 205 (2013).

[32] B. Vlastakis, G. Kirchmair, Z. Leghtas, S. E. Nigg, L. Frunzio, S. M. Girvin, M. Mirrahimi, M. H. Devoret, and R. J. Schoelkopf, Science **342**, 607 (2013).

[33] A. Luis, Phys. Rev. A **69**, 044101 (2004).

[34] M. J. W. Hall, D. W. Berry, M. Zwierz, and H. M. Wiseman, Phys. Rev. A **85**, 041802 (2012).

[35] K. McKenzie, D. A. Shaddock, D. E. McClelland, B. C. Buchler, and P. K. Lam, Phys. Rev. Lett. **88**, 231102 (2002).

[36] J. Miller, L. Barsotti, S. Vitale, P. Fritschel, M. Evans, and D. Sigg, Phys. Rev. D **91**, 062005 (2015).

[37] F. Toscano, D. A. R. Dalvit, L. Davidovich, and W. H. Zurek, Phys. Rev. A **73**, 023803 (2006).

[38] D. A. R. Dalvit, R. L. de Matos Filho, and F. Toscano, New J. Phys. **8**, 276 (2006).

[39] S. Mancini, V. I. Man'ko, and P. Tombesi, Phys. Rev. A **55**, 3042 (1997).

[40] S. Bose, K. Jacobs, and P. L. Knight, Phys. Rev. A **56**, 4175 (1997).

[41] K. Jacobs, *Quantum Measurement Theory and Its Applications* (Cambridge University Press, Cambridge, 2014).

[42] D. Vion, A. Aassime, A. Cottet, P. Joyez, H. Pothier, C. Urbina, D. Esteve, and M. H. Devoret, Science **296**, 886 (2002).

[43] J. Koch, T. M. Yu, J. Gambetta, A. A. Houck, D. I. Schuster, J. Majer, A. Blais, M. H. Devoret, S. M. Girvin, and R. J. Schoelkopf, Phys. Rev. A **76**, 042319 (2007).

[44] K. M. Sliwa, M. Hatridge, A. Narla, S. Shankar, L. Frunzio, R. J. Schoelkopf, and M. H. Devoret, Phys. Rev. X **5**, 041020 (2015).

[45] F. Lecocq, L. Ranzani, G. A. Peterson, K. Cicak, R. W. Simmonds, J. D. Teufel, and J. Aumentado, Phys. Rev. Appl. **7**, 024028 (2017).

[46] R. W. Andrews, A. P. Reed, K. Cicak, J. D. Teufel, and K. W. Lehnert, Nat. Commun. **6**, 10021 (2015).

[47] A. P. Reed, K. H. Mayer, J. D. Teufel, L. D. Burkhart, W. Pfaff, M. Reagor, L. Sletten, X. Ma, R. J. Schoelkopf, E. Knill, and K. W. Lehnert, arXiv:1703.02548.

[48] W. Pfaff, C. J. Axline, L. D. Burkhart, U. Vool, P. Reinhold, L. Frunzio, L. Jiang, M. H. Devoret, and R. J. Schoelkopf, Nat. Phys. (2017), doi:10.1038/nphys4143.

[49] A. A. Clerk, F. Marquardt, and K. Jacobs, New J. Phys. **10**, 095010 (2008).

[50] C. W. Gardiner and M. J. Collett, Phys. Rev. A **31**, 3761 (1985).

[51] H. M. Wiseman, Ph.D. dissertation, The University of Queensland, Brisbane, 1994.